



CHALMERS
UNIVERSITY OF TECHNOLOGY

Techno-economic assessment of fluidized bed calcium looping for thermochemical energy storage with CO₂ capture

Downloaded from: <https://research.chalmers.se>, 2023-05-06 06:27 UTC

Citation for the original published paper (version of record):

Martinez Castilla, G., Guío-Pérez, D., Papadokonstantakis, S. et al (2021). Techno-economic assessment of fluidized bed calcium looping for thermochemical energy storage with CO₂ capture. Short papers from the 11th International Trondheim CCS Conference: 390-397

N.B. When citing this work, cite the original published paper.

TECHNO-ECONOMIC ASSESSMENT OF FLUIDIZED BED CALCIUM LOOPING FOR THERMOCHEMICAL ENERGY STORAGE WITH CO₂ CAPTURE

Guillermo Martinez Castilla*, Diana Carolina Guio-Pérez, Stavros Papadokonstantakis, David Pallarès, Filip Johnsson

Chalmers University of Technology, Gothenburg, Sweden

* Corresponding author e-mail: castilla@chalmers.se

Abstract

The multicyclic carbonation-calcination of CaCO₃ in fluidized bed reactors is a promising process for both thermochemical energy storage (TCES) and CO₂ capture. In this paper, a techno-economic assessment of the calcium loop (CaL) process with simultaneous TCES and CO₂ capture from an existing CO₂-emitting facility is carried out. Inputs to the process are non-dispatchable high temperature heat and a stream of flue gas, while the process outputs are electricity (both dispatchable and non-dispatchable) and CO₂ for compression and storage. The process is sized so the charging section can run steadily during 12h per day and the discharging section to operate steadily 24h per day. The study assesses the economic performance of the process through the breakeven electricity price (BESP) and cost per CO₂ captured. The study excludes the costs of the renewable energy plant and the CO₂ transport and storage. The sensitivity of the results to the main process and economic parameters is also assessed. Results show that the BESP of the case with the most realistic set of economic predictions ranges between 141 and -20 \$/MWh for varying plant size. When assessed as a carbon capture facility with a revenue made from both the electricity sale and the carbon capture services, the cost ranges between 178 and 4 \$/tCO₂-captured. The investment cost of the reactors is found to be the largest fraction of the computed costs, while the sensitivity analysis points at the degree of conversion in the carbonator as the most crucial parameter, with large cost reductions for increased conversion.

Keywords: solid cycles, heat to power, dispatchability, storage cost

1. Introduction

Anthropogenic carbon dioxide (CO₂) emissions represent the main cause of climate change [1]. Despite the continuous efforts in the deployment of renewable energy generation technologies to replace fossil fuels [2], the increasing energy demand has made the share of fossil fuel in the primary energy demand to remain constant at 80% [3] and thereby the global CO₂ emissions have kept growing [4] (yet with a reduction during 2020 due to the reduced economic activity resulting from the Covid pandemic). A large share of the renewable expansion during the last decades have been in the form of wind and solar power, driven by large reductions in costs for these technologies. Due to the variability of wind and solar power generation, their value to the electricity system is reduced as their share in the system increases [5] as well as they may cause instabilities in the grid [6]. Thus, to maintain the value of wind and solar, different forms of energy storage and flexibility measures need to be implemented. There are different forms of storage such as batteries, pumped hydro and thermal energy storage can all have their role in the energy system. Of particular importance is storage which is able to handle variations of several days or weeks corresponding to the time characteristics of wind power. Thermochemical energy storage (TCES) is gaining special attention since, compared to thermal energy storage (TES), TCES displays larger energy density [7] as well as the possibility for long term storage and shipping [8]. Among other alternatives, gas-solid cycles are the most promising TCES systems due to their high reversibility, stability, and enthalpy of reaction. Although packed beds (moving or stationary) have been typically used for investigations of TCES through solids cycling at bench-, lab- and pilot-scale [9], fluidized beds should be an efficient reactor

technology for commercial-scale due to the significantly higher mixing required in larger units.

In addition, to increased share of renewable energy most future scenarios which comply with the Paris Agreement includes substantial amounts of carbon capture and storage (CCS) [10]. Several CCS technologies have been investigated and tested, with a special focus on post-combustion systems. The energy penalty associated to the operation of these processes remains however the major drawback in the commercial deployment of CCS [11].

The calcium looping (CaL) process has been investigated both as a CCS and a TCES technology, indicating that it can potentially be of double use in the energy transition [2]. The CaL process is based on the multicyclic calcination-carbonation of CaCO₃, which can be obtained from limestone, a cheap and abundant material. Thus, it is based on the following reactions:



When applied for CO₂ capture, the CaL process represents a promising capture technology with respect to efficiency and costs [12]. If implemented as TCES, it increases the dispatchability of renewable energy facilities able to provide high-temperature streams such as concentrated solar power (CSP) plants [13], [14]. In addition, if the TCES facility is installed close to a CO₂ emitting source, the CaL process could simultaneously produce dispatchable electricity while mitigating atmospheric CO₂ emissions from the nearby source. A review of the implications of the CaL process scale-up for both CO₂ capture and TCES applications has recently been

published by Ortiz et al. [15], including an analysis of different gas-solid reactor systems. When it comes to the TCES-CSP application, Ortiz et al. [13] published an in-depth review of different process schemes, conditions and materials advantageous for the operation. Bayon et al. [16] provide a techno-economic comparison of 17 gas-solid TCES systems (excluding the reactors), computing a CaL-TCES cost of 54 \$/kWh, (note that this cost is expressed per storage capacity) as compared to the cost estimated by Muto et al. [17] for a CaL-TCES process using a synthetic sorbent; 56-59 €/MWh. Nevertheless, studies on the costs associated to the CaL-TCES process are scarce due to the early stage of development [18], [19] and, thus, they are often based on the more abundant cost studies of the more mature CaL process as CO₂ capture technology (see [20] for an overview). Among these, it is worth mentioning the work by Michalski et al. [21], where a method for assessing the economic feasibility of CaL-CCS processes was suggested based on commercial technology appraisal tools. According to another study by Mantripragada et al. [22] the reactors represent the largest cost of the CaL plant together with the solids handling.

In summary, although the economic feasibility of the CaL process has been widely studied for CO₂ capture, there is little work when it comes to assess the economics of applying it as a

2. Process description

The present section describes the CaL process scheme used for the current investigation. The work by Chacartegui et al. [23] has been used as the basis for the study, i.e. adapting the process layout, although some process conditions have been modified and additional assumptions have been made according to the nature of the present work (i.e. combined TCES and CO₂ capture). Furthermore, the process scheme considers fluidized beds for both the carbonator and calciner reactors, which adds some requirements related to the presence of fluidization agents. The energy input to the process is assumed to come from a renewable energy source capable to provide high temperature heat intermittently, e.g. a concentrated solar power collector. Figure 1 shows a schematic representation of the process studied in this work. The charging and discharging sections can be operated independently. Correspondingly, solids storage at ambient conditions is considered for both charged and discharged particles, which, although decreasing the process efficiency, allows the potential introduction of shipping and make-up streams to the process without altering the thermodynamic performance. Yet, although shipping of the solids would allow the more efficient use of non-dispatchable sources, it is left outside the scope of the present work.

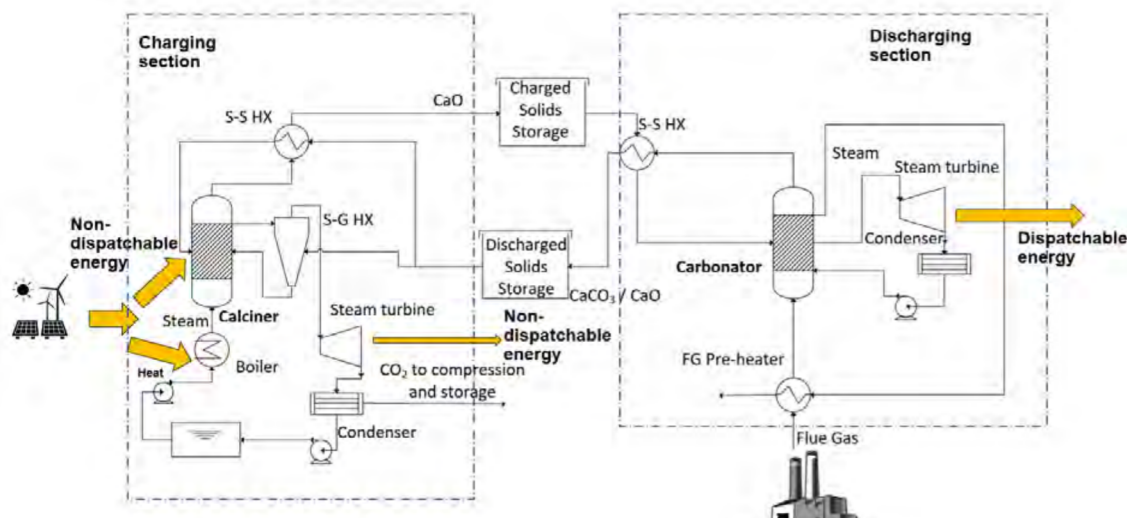


Figure 1. Schematic diagram of the investigated process. Note that the non-dispatchable energy input is in the form of high-temperature heat and the produced energy is in the form of electricity.

TCES scheme, especially when combined with CO₂ capture. Thus, the aim of this work is to estimate the cost of the CaL process when deployed for TCES in a renewable energy generation facility and combined with the capture of the CO₂ emitted by an existing facility located nearby (i.e. not accounting for transportation and storage of CO₂). Such scenario is motivated by the need of combustion facilities to operate until the initial investment is paid-off, which under an increasing cost for CO₂ emissions, will require the capture of the emitted CO₂. The process scheme here presented is developed taking a previous thermodynamic study on CaL for TCES [23] as starting point, and adapting the process for the integration of carbon capture. The cost of the process is calculated through a bottom-up approach and presented in the form of breakeven electricity selling price (BESP) and per CO₂ captured. The sensitivity of the computed cost to process size, material degree of conversion and income associated to the CO₂ captured and electricity sales is also investigated.

Energy in the form of heat at high temperature (850 °C, see below) is used to run the charging section, comprised by the calcination reactor and a steam generator that evaporates and superheats steam for fluidizing the reactor. As reported in [24], calcination under superheated steam decreases the temperature required for calcination and increases the conversion of the solids in the carbonation side. Lower calcination temperatures are desired since simpler and cheaper energy collectors can be utilized [13]. In this work the calciner conditions have been fixed to 850 °C and 1 bar, following the conclusions from [13]. The gas stream exiting the calcination reactor (consisting mainly of H₂O and CO₂) is used to preheat part of the total inflow of discharged solids (with the split fraction taken from [23]) and is subsequently expanded in a turbine down to the condensing pressure (set by the cooling water temperature), enabling also the separation of steam and leaving the carbon dioxide ready for compression. A water tank allows the feedwater to be stored when the calciner is not in operation. The process incorporates two solid-solid heat exchangers to preheat the feeding solids with the hot streams leaving the reactors.

The energy discharging is achieved with the use of a Rankine cycle that runs the dispatchable steam turbine using the heat released in the carbonator reactor, which is fluidized with the flue gas from a nearby facility. This condition sets the carbonation conditions of the investigated process to 650 °C and 1 bar. Since the optimization of the process performance falls outside the scope of this work, a simplistic approach has been followed for the power cycle conditions. Steam at 550 °C and 120 bar is generated and expanded in one step to condensing pressure. Note that pre-heating of the feedwater line has been left out of the study.

3. Methodology

3.1 Mass and energy balances

In order to carry out the economic assessment of the process defined in Section 2 including both the capital and operational costs of the plant, a thermodynamic analysis is performed, followed by the computation of mass and energy balances and the corresponding equipment sizing. Table 1 presents the values of process parameters assumed in this study and referred in the following sections as the base case. A charging time t_{charge} is defined as the hours per day that the charging side is assumed to be running, i.e. when the intermittent renewable energy source can be harnessed and has been fixed to 12h. Thus, the storage is sized to provide the amount of charged solids (CaO) required to run the discharging side during 24- t_{charge} hours per day. The calciner is sized so it can convert the available heat input Q_{calc} into stored chemical energy while the carbonator is sized to operate continuously.

Both reactors are computed as stirred tank reactors, with all output streams leaving at the reactor temperature. The flue gas entering the process is assumed to contain 15% of CO₂ and the capture rate in the carbonator has been fixed to 90% according to [25]. All gas flows are assumed ideal and no pressure drop calculations are included in the study. Each solid-solid heat exchanger (SS-HX) is computed as a series of two bubbling fluidized bed solid-gas heat exchangers, whose volumes are estimated based on the heat-transfer coefficient reported in [26]. The solid-gas heat exchangers (SG-GX) are in turn sized as cyclones [27] according to the method available at [28], while solid storage tanks are sized using the method suggested by Bayon et al. [16]. No solid losses in cyclones and fluidized beds have been accounted. The rest of conventional fluid-fluid heat exchangers have been sized using heat transfer coefficients from [29].

Table 1. Main process assumptions and parameters of the base case. Values with (*) are modified in the sensitivity analysis (Section 4).

| Parameter | Value | Unit |
|---|----------|--------------------|
| Plant size as net heat input into the process, Q_{in} | 100 (*) | MW |
| Percentage of steam in the calciner | 50 | % |
| Charging time, t_{charge} | 12 | h |
| Storage temperature | 20 | °C |
| Cooling water temperature | 20 | °C |
| Minimum temperature difference SS-HX | 20 | °C |
| Minimum temperature difference SG-HX | 15 | °C |
| Minimum temperature difference condensers | 15 | °C |
| S-G heat transfer coefficient | 480 | W/m ² K |
| Fluid-fluid heat transfer coefficients | 1500 | W/m ² K |
| Flue gas CO ₂ content | 15 | %v |
| Capture rate | 90 | % |
| Available cooling water discharge temperature | 70 | °C |
| Cooling water pumping distance (m) | 1000 | m |
| Solids porosity, Φ | 0.5 | - |
| Turbomachinery isentropic efficiency, η_{is} | 0.89 | - |
| Fraction of discharged solids preheated in the SS-HX | 0.85 | - |
| Conversion in the calciner, x_{calc} | 1 | - |
| Conversion in the carbonator, x_{carb} | 0.25 (*) | - |
| Solids conveying energy requirement | 10 | MJ/t/100m |
| Equivalent solids conveying length | 100 | m |

3.2 Economic assessment

The assessment of the economic performance of the plant is done using as indicator the break-even electricity selling price (BESP). This is computed by setting the calculated net present value (NPV) of the plant to zero, i.e. calculating an electricity selling price such that the revenues balance the cost over the lifetime of the plant. Thus, the NPV is computed in this work as the sum of the discounted annual cash flows during the lifetime of the project, see Equation 3.

$$NPV = \sum_{i=1}^n \frac{CF_i}{(1+r)^i} \quad (3)$$

A bottom-up approach is used to compute the annual cash flows, i.e. breaking down the plant costs into basic components and subsequently adding installation and indirect costs. The total plant cost methodology followed in this work is based on [30]. Table 2 shows the cost functions used to estimate the erected cost of each process component, which are based on the cost of a reference component of size S_0 and scaled through the scaling parameter f (Equation 4):

$$C = C_0 \left(\frac{S}{S_0} \right)^f \quad (4)$$

Although several works [31],[32] have focused on the calciner reactor design that would allow the heat transfer from the CSP plant, this is assumed to be outside of the scope of this work and instead the calciner cost is estimated based on an oxy-circulating fluidized bed (CFB) furnace reference cost [33], assuming the heat transfer surfaces are used to add heat into the reactor. Similarly, the carbonator is assumed to be similar to a conventional CFB-boiler [33]. Due to lack of available data, the cost of solid-solid heat exchangers is estimated as two times the cost of a bubbling fluidized bed dryer. The only liquid vessel

present in the process (to store the feedwater in the charging side) is assumed cylindrical and similar to standard water vessels [34], with a total specific cost of 83 \$/m³ [16].

Table 2. Capital cost functions (in M\$) used in the study

| Equipment | Cost function | Reference |
|----------------------------|---|-----------|
| Calciner | $C = 5.87 \cdot 10^2 \cdot \left(\frac{Q_{in}}{2514}\right)^{0.67}$ | [33] |
| Carbonator | $C = 5.60 \cdot 10^2 \cdot \left(\frac{Q_{out}}{1521}\right)^{0.67}$ | [33] |
| Solid-gas heat exchanger | $C = 3.98 \cdot 10^{-9} \cdot D_{cyc}^2 + 2.73 \cdot 10^{-6} \cdot D_{cyc} + 0.016$ | [27] |
| Solid-solid heat exchanger | $C = 2 \cdot 3.5 \cdot 10^{-1} \cdot \left(\frac{D_b \cdot u_g}{2}\right)^{0.73}$ | [29] |
| Gas-gas heat exchanger | $C = (2546.9 \cdot A_{HX}^{0.67} \cdot P_{gas}^{0.28}) \cdot 10^{-6}$ | [21] |
| Cooler | $C = (2546.9 \cdot A_{HX}^{0.67} \cdot P_{fluid}^{0.28}) \cdot 10^{-6}$ | [21] |
| Solids Storage | $C = V_{steel} \cdot C_{steel}$ | [16] |
| Steam turbine | $C = 473 \cdot 10^{-6} \cdot \left(\frac{W_{turb}}{25}\right)^{0.67}$ | [35] |
| Electric generator | $C = 84.5 \cdot 10^{-6} \cdot (P_{el} \cdot 10^3)^{0.95}$ | [21] |
| Steam generator | $C = 2.85 \cdot \left(\frac{\dot{m}_{steam}}{14}\right)^{0.35}$ | [29] |
| Pump | $C = \left(\frac{P_{el}}{197}\right)^{0.60}$ | [21] |

The values selected for the key economic parameters assumed in this work are listed in Table 3. The income received for capturing the CO₂ of a nearby facility (*IncomeCC*) has been taken as 50 \$/ton, which is the estimated cost for capturing CO₂ from a flue gas stream as the one included here [36]. The CO₂ compression and storage are not included in the study since their cost would be transferred to the emitting industry and are therefore not considered to play a role in the process feasibility. Moreover, the cost of the renewable energy input has also been left out since it is assumed not to be part of the cost of the storage technology here investigated. Lastly, the make-up and purge/loss of solid material has been neglected.

Table 3. Main assumptions and input data for the economic analysis. Values with (*) are modified in the sensitivity analysis (Section 4).

| Parameter, Unit | Value |
|---|--------|
| Plant lifetime (years) | 20 |
| Capacity factor (%) | 100 |
| Discount rate (%) | 4.75 |
| Limestone cost (\$/ton) | 10 |
| Carbon capture-derived income, <i>IncomeCC</i> (\$/ton) | 50 (*) |
| Electricity selling price, <i>ESP</i> (\$/MWh) | 40 (*) |

In order to compare the process cost with other CO₂ capture technologies the total cost of the plant is also expressed in the typical capture cost metric, \$/tCO₂-captured (note that this is done only to allow the comparison, since the CO₂ capture is treated in this study as an income cashflow and therefore it is not an actual cost). To do so, the NPV includes the selling of the generated electricity and the revenue obtained for the CO₂ capture as positive cashflows. For this, the electricity is assumed to be sold at a price of 40 \$/MWh in the base case [37].

To scrutinize the economic assessment of the process, a sensitivity analysis has been carried out. Firstly, the impact of size has been evaluated, varying the instantaneous net energy input from 50 to 1000 MW. Secondly, since often reported as a crucial limiting performance parameter [38], [15], the effect of the degree of conversion of the solids in the carbonator has been investigated. Lastly, the value for the income stream associated to carbon capture has been varied from 10 to 100 \$/tCO₂ captured, which is directly related to the forecasted cost of emitting CO₂, whereas the assumed electricity selling price (*ESP*) has been varied from 20 to 80 \$/MWh.

4. Results and discussion

Figure 2 presents the simplified energy flow calculated for the base case process (see Table 1). The top scheme illustrates the energy distribution when the charging side is operating (renewable energy source is available), while the bottom diagram shows the energy flows when only the discharging side operates. It can be noted that the efficiency of the base process on a heat-to-dispatchable power is rather low (28%) mostly due to the heat lost in the condensers, in the solids storage and the heat exchanger losses connected to the high amount of inactive solids due to the low conversion efficiency in the carbonator ($x_{carb}=0.25$ for the base case). This is partially due to that the process is far from being optimized, with the two power blocks defined as basic Rankine cycles. Literature studies have shown that the efficiency of the optimized process (for the TCES scheme) can reach up to 45% [39], [23]. Also, the vast majority of the losses are in the form of heat, and this work does not assess the possibility to include heat streams in the product portfolio of the plant (in the form of district or industrial heating), in which case some part of this loss would turn into a revenue stream. It is worth pointing out that the use of superheated steam to fluidize the calciner implies an added energy loss in the steam generator that is partly recovered in the non-dispatchable turbine, which produces most of the energy when the charging side is in operation. Varying the percentage of steam in the calciner (0.5 has been used in the base case) has an impact on the total energy output shares, with lower steam contents increasing the dispatchability of the process, i.e. the weight of the dispatchable turbine on the total energy output increases.

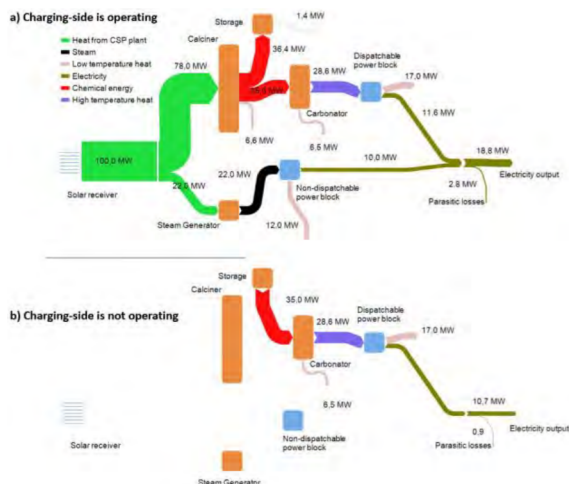


Figure 2. Simplified energy flow of the process for the base case when (a) both charging and discharging side are operating and (b) when the calciner is not operating. Note that the scheme has been simplified and recycle streams are not presented here, as well as some of the losses have been merged.

Figure 3 maps the total plant cost disclosure for different net energy inputs. It is seen that the reactors represent the main fraction of the total cost, especially at larger sizes (i.e. over 80% of the total cost for the 1000-MW case against 75% for the 50-MW case), which is in line with the study in [22]. Note that in the present work the reactor costs also include heat transfer surfaces, both for transferring heat into the calciner and for steam generation and superheating in the carbonator. These results highlight the importance of reactor costing when assessing TCES processes, which should be borne in mind when choosing a specific reactor type and design [13]. The heat exchangers and fixed operational and maintenance (O&M) costs are the second and third largest expenses, respectively, with the latest gaining weight at larger plant sizes since they scale-up linearly while the heat exchangers capital cost is favored by the economy of scale.

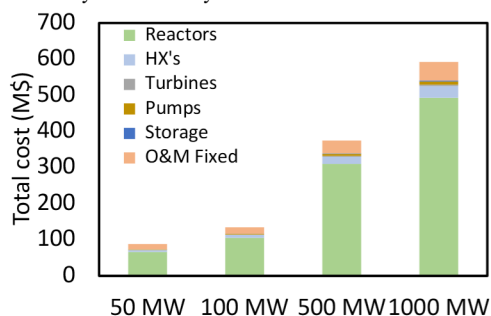
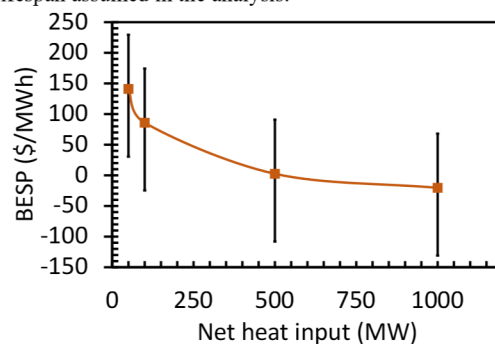


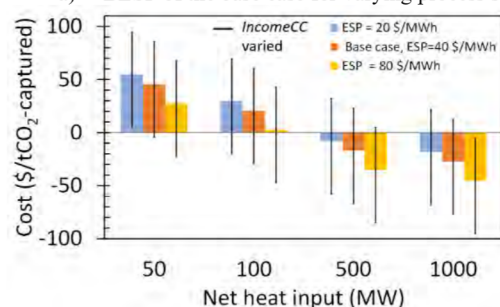
Figure 3. Disclosure of the total costs (in M\$) of the base case process for different net heat input

As expected, the BESP decreases with process size, as seen in Figure 4a, ranging from 141 \$/MWh for the smaller size to -20 \$/MWh for the 1 GW case (all other process parameters were fixed to the base case values). Note that a negative BESP indicates that the process would be profitable with only the income connected to the carbon capture services. A similar trend is observed when the cost is expressed as \$/tCO₂-captured, ranging between 45 and -27 \$/tCO₂-captured. The figure shows that the cost variation is steeper in the range 0-500 MW, becoming less sensitive in the 500-1000 MW range. In order to quantify the impact of the revenue stream related to

CO₂ capture, the base case assumption of *IncomeCC* (50 \$/tCO₂-captured) has been changed and the variation has been plotted as vertical error bars (10 to 100 \$/tCO₂) in Figure 4. It can be seen that the net impact on the cost is constant with size, which is caused by the fact that the amount of CO₂ captured scales linearly with the net heat input. Consequently, the income associated to the CO₂ capture has a stronger influence on the total plant economics at larger sizes. When the assumed electricity selling price (ESP) used for the computation of the capture cost is varied, it is observed in Figure 4b that for most of the cases the plant would breakeven before the 20 years lifespan assumed in the analysis.



a) BESP of the base case for varying process size



b) \$/tCO₂-capture for varying process size and electricity selling price (ESP)

Figure 4. Computed plant cost of the base case process for different sizes when a) expressed as BESP (\$/MWh) and b) expressed as capture cost (\$/tCO₂ captured) for different electricity selling prices (ESP). The vertical error bars represent the sensitivity of the cost to the assumption of income related to CO₂ capture IncomeCC (considered to range from 10 to 100\$/tCO₂).

The main results from varying the material degree of conversion in the carbonator to evaluate the impact on the plant costs are presented in Figure 5, both in terms of BEP (Figure 5a) and \$/tCO₂-captured (Figure 5b). Note that the size of the process, the CO₂ capture income and electricity price assumptions have been fixed to their base case values (100 MW, 50 \$/tCO₂ and 40 \$/MWh respectively). The relatively strong impact of x_{carb} on the plant cost can be confirmed with reductions on the BEP of 24 \$/MWh when x_{carb} is increased from 0.15 to 0.25, although it becomes less prominent for $x_{carb} > 0.5$. This impact is also noticeable when the cost is expressed in terms of captured CO₂, where low carbonation degrees yield higher capture costs.

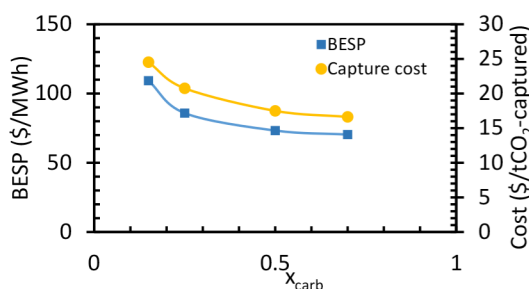


Figure 5. Sensitivity of the plant cost for different material reactivities in the carbonator when expressed as BESP (\$/MWh) and as \$/tCO₂ captured. All other process parameters are set according to the base case

It is important to mention that the critical importance of the material conversion on the process performance and had previously been identified by several authors [15], although not for a system like the one presented here and not in terms of economic performance. Though important for most of the TCES solid-gas systems [9], this parameter gains special relevance in the CaL process since its value can change by a factor of 2.5 depending on the reactor conditions [13] and whether the process is designed for TCES-only or for TCES-CCS like the one here presented. These findings highlight the need for material developments for successful deployment of the CaL process.

If the energy source is a solar receiver characteristic of CSP plants, its cost and design are other aspects that need to be addressed in more detailed economic assessments of the process here presented. The calciner conditions chosen in this work (850 °C) allow the use of cheaper equipment but the impact of such cost on the overall techno-economic performance is still unknown.

The results of the current work can be compared to other energy storage processes through the BESP as well as to other CO₂ capture systems through the cost expressed in \$/tCO₂-captured. As examples of the former, Ganwal et al. [17] reported a cost of 56-59 \$/MWh for a CaL storage process with a synthetic material of $x_{carb} = 0.4$, which would be comparable to the cost obtained in this work (see Figure 5a). Michalski et al. [21] reported a levelized cost of electricity (LCOE) of 80-95 \$/MWh, although their result is for retrofitting a coal power plant. Cormos [40] also carried out a retrofitting study concluding that the LCOE of a retrofitted CaL-power plant would range from 68-74 \$/MWh. Some of the main publications addressing the cost of CaL-CCS [20] report a cost range of 20-40 \$/ tCO₂-captured, which is comparable to the computed costs in this work for carbonation reactivities higher than 0.5. Furthermore, the work published by MacKenzie et al. [41] state that the cost was mostly sensitive to the material deactivation and limestone cost. Although neglected in the present work, these factors could play important roles in the long-term, given the low degree of solids conversion in CCS applications [15].

5. Conclusions

A techno-economic investigation of a fluidized-bed calcium looping process for both thermochemical energy storage and CO₂ capture is presented. The process layout used for the current study is based on state-of-the-art literature works on the CaL process and is applied under the assumption that high temperature heat provided by renewables such as from a concentrated solar power plant is available intermittently. Such heat is used to feed the charging section (calcination) and dispatchable electricity is produced in the discharge section while capturing CO₂ from an existing emitting facility nearby.

A bottom-up approach is used to compute the electricity price that would make the process viable as well as the cost expressed by means of captured CO₂.

The analysis points at the investment costs of the reactors as the major costs of the process, which indicates that the overall cost of the process would not vary much when handling storage times larger than the ones considered here. For the conditions investigated, the calculated BESP ranges from 141 to -20 \$/MWh for the 50-1000 MW size span, which corresponds to 45 and -27 \$/ tCO₂-captured. A sensitivity analysis shows that these numbers are lowered with increasing future carbon prices and with an increased degree of conversion in the carbonator. The latest is found to play a large role on the techno-economic performance, since it affects both the process energy flow and the amount of CO₂ captured and consequently the side-revenue of the process. The study also shows the importance of further analysis and optimization when it comes to choosing optimal conditions in the reactors and concentration of fluidization gas. Note that for the sake of simplicity, the results shown here do not include the cost of the renewable energy input nor the revenues associated to the heat streams.

Future work includes the optimization of the current setup and the subsequent evaluation of parameters such as reactors conditions and mechanical properties of the solids, which requires more advanced process and reactor models. Especially when it comes to evaluate the flexible operation of the charging process in the presence of various intermittent sources, dynamic models capable to describe the transient operation are required, allowing the computation of start-up and shut off times as well as investigation of different control strategies.

References

- [1] T.F. Stocker, D. Quin, IPCC 2013: CLIMATE CHANGE 2013 - The Physical Science Basis, Contribution of Working Group I to the Fifth Assessment Report of the Intergovernmental Panel on Climate Change, Cambridge University Press, 2013. <https://doi.org/10.1017/CBO9781107415324.Summary>.
- [2] International Renewable Energy Agency, IRENA (2019), Global Energy Transformation: A Roadmap to 2050, 2019. <https://www.irena.org/publications/2019/Apr/Global-energy-transformation-A-roadmap-to-2050-2019Edition>.
- [3] F. Johnsson, J. Kjärstad, J. Rootzén, The threat to climate change mitigation posed by the abundance of fossil fuels, Clim. Policy. 19 (2019) 258–274. <https://doi.org/10.1080/14693062.2018.1483885>.
- [4] IEA, World Energy Outlook (2020), Paris, 2020. <https://www.iea.org/reports/world-energy-outlook-2020>.
- [5] L. Hirth, The market value of variable renewables. The effect of solar wind power variability on their relative price, Energy Econ. 38 (2013) 218–236. <https://doi.org/10.1016/j.eneco.2013.02.004>.
- [6] J.G.L.G.S.N.M.B. David Steen, Challenges of integrating solar and wind into the electricity grid, (2014) 94. <http://publications.lib.chalmers.se/publication/210515-challenges-of-integrating-solar-and-wind-into-the-electricity-grid>.
- [7] P. Pardo, A. Deydier, Z. Anxionnaz-Minvielle, S. Rougé, M. Cabassud, P. Cognet, A review on high temperature thermochemical heat energy storage, Renew. Sustain. Energy Rev. 32 (2014) 591–610. <https://doi.org/10.1016/j.rser.2013.12.014>.
- [8] J. Sunku Prasad, P. Muthukumar, F. Desai, D.N. Basu, M.M. Rahman, A critical review of high-temperature reversible thermochemical energy storage systems, Appl.

- Energy. 254 (2019) 113733.
<https://doi.org/10.1016/j.apenergy.2019.113733>.
- [9] A.J. Carrillo, J. González-Aguilar, M. Romero, J.M. Coronado, Solar Energy on Demand: A Review on High Temperature Thermochemical Heat Storage Systems and Materials, *Chem. Rev.* 119 (2019) 4777–4816.
<https://doi.org/10.1021/acs.chemrev.8b00315>.
- [10] IEA, CCUS in Clean Energy Transitions, Paris, 2020.
<https://www.iea.org/reports/ccus-in-clean-energy-transitions>.
- [11] M.E. Boot-Handford, J.C. Abanades, E.J. Anthony, M.J. Blunt, S. Brandani, N. Mac Dowell, J.R. Fernández, M.C. Ferrari, R. Gross, J.P. Hallett, R.S. Haszeldine, P. Heptonstall, A. Lyngfelt, Z. Makuch, E. Mangano, R.T.J. Porter, M. Pourkashanian, G.T. Rochelle, N. Shah, J.G. Yao, P.S. Fennell, Carbon capture and storage update, *Energy Environ. Sci.* 7 (2014) 130–189.
<https://doi.org/10.1039/c3ee42350f>.
- [12] M. Zhao, A.I. Minett, A.T. Harris, A review of techno-economic models for the retrofitting of conventional pulverised-coal power plants for post-combustion capture (PCC) of CO₂, *Energy Environ. Sci.* 6 (2013) 25–40.
<https://doi.org/10.1039/c2ee22890d>.
- [13] C. Ortiz, J.M. Valverde, R. Chacartegui, L.A. Pérez-Maqueda, P. Giménez, The Calcium-Looping (CaCO₃/CaO) process for thermochemical energy storage in Concentrating Solar Power plants, *Renew. Sustain. Energy Rev.* 113 (2019) 109252.
<https://doi.org/10.1016/j.rser.2019.109252>.
- [14] A.A. Khosa, T. Xu, B.Q. Xia, J. Yan, C.Y. Zhao, Technological challenges and industrial applications of CaCO₃/CaO based thermal energy storage system – A review, *Sol. Energy.* 193 (2019) 618–636.
<https://doi.org/10.1016/j.solener.2019.10.003>.
- [15] C. Ortiz, J. Manuel Valverde, R. Chacartegui, L.A. Pérez-Maqueda, P. Gimenez-Gavarrell, Scaling-up the Calcium-Looping Process for CO₂ Capture and Energy Storage, *KONA Powder Part. J.* (2021) 1–20.
<https://doi.org/10.14356/kona.2021005>.
- [16] A. Bayon, R. Bader, M. Jafarian, L. Fedunik-Hofman, Y. Sun, J. Hinkley, S. Miller, W. Lipiński, Techno-economic assessment of solid–gas thermochemical energy storage systems for solar thermal power applications, *Energy.* 149 (2018) 473–484.
<https://doi.org/10.1016/j.energy.2017.11.084>.
- [17] A. Muto, T. Hansen, Demonstration of high-temperature calcium-based thermochemical energy storage system for use with concentrating solar power facilities, 2018.
<https://www.osti.gov/servlets/purl/1523643>.
- [18] Socratces Project, (2021). <https://socratces.eu/>.
- [19] G. Flamant, H. Benoit, M. Jenke, A.F. Santos, S. Tescari, G. Moumin, A. Rodriguez, A. Azapagic, L. Stamford, J. Baeyens, Y. Boes, F. Pron, M. Prouteau, P. Dumont, N. Abdenouri, H. Mazouz, Solar processing of reactive particles up to 900°C, the SOLPART project, *AIP Conf. Proc.* 2033 (2018). <https://doi.org/10.1063/1.5067013>.
- [20] P. Fenell, B. Anthony, Calcium and Chemical Looping Technology for Power Generation and Carbon Dioxide (CO₂) Capture, Woodhead Publishing Series, Cambridge, 2015.
- [21] S. Michalski, D.P. Hanak, V. Manovic, Techno-economic feasibility assessment of calcium looping combustion using commercial technology appraisal tools, *J. Clean. Prod.* 219 (2019) 540–551.
<https://doi.org/10.1016/j.jclepro.2019.02.049>.
- [22] H.C. Mantripragada, E.S. Rubin, Calcium looping cycle for CO₂ capture: Performance, cost and feasibility analysis, *Energy Procedia.* 63 (2014) 2199–2206.
<https://doi.org/10.1016/j.egypro.2014.11.239>.
- [23] R. Chacartegui, A. Alovio, C. Ortiz, J.M. Valverde, V. Verda, J.A. Becerra, Thermochemical energy storage of concentrated solar power by integration of the calcium looping process and a CO₂ power cycle, *Appl. Energy.* 173 (2016) 589–605.
<https://doi.org/10.1016/j.apenergy.2016.04.053>.
- [24] S. Champagne, D.Y. Lu, A. MacChi, R.T. Symonds, E.J. Anthony, Influence of steam injection during calcination on the reactivity of CaO-based sorbent for carbon capture, *Ind. Eng. Chem. Res.* 52 (2013) 2241–2246.
<https://doi.org/10.1021/ie3012787>.
- [25] Y.A. Criado, B. Arias, J.C. Abanades, Calcium looping CO₂ capture system for back-up power plants, *Energy Environ. Sci.* 10 (2017) 1994–2004.
<https://doi.org/10.1039/c7ee01505d>.
- [26] F. Scala, Fluidized bed technologies for near-zero emission combustion and gasification, Woodhead Publishing Series, Cambridge, 2013.
- [27] E. De Lena, M. Spinelli, M. Gatti, R. Scaccabarozzi, S. Campanari, S. Consonni, G. Cinti, M.C. Romano, Techno-economic analysis of calcium looping processes for low CO₂ emission cement plants, *Int. J. Greenh. Gas Control.* 82 (2019) 244–260.
<https://doi.org/10.1016/j.ijggc.2019.01.005>.
- [28] U. MUSCHELKNAUTZ, E. MUSCHELKNAUTZ, Abscheideleistung von Rückführzyklonen in Wirbelschichtfeuerungen, *VGB Kraftwerkstechnik.* 79 (1999) 58–63.
- [29] R.D. Woods, Rules of Thumb in Engineering Practice, Wiley-VCH, Weinheim, 2007.
- [30] G. Manzolini, E. MacChi, M. Gazzani, CO₂ capture in Integrated Gasification Combined Cycle with SEWGS - Part B: Economic assessment, *Fuel.* 105 (2013) 220–227.
<https://doi.org/10.1016/j.fuel.2012.07.043>.
- [31] DOE/NETL, Cost and Performance for Low-Rank Pulverized Coal Oxycombustion Energy Plants, *Tech. Rep.* (2010) 442.
<https://www.globalccsinstitute.com/archive/hub/publications/119786/cost-performance-low-rank-pulverized-coal-oxycombustion-energy-plants.pdf>.
- [32] S. Walas, Chemical Process Equipment, Elsevier, 1988.
<https://doi.org/https://doi.org/10.1016/C2009-0-25916-2>.
- [33] A. Pizzolato, F. Donato, V. Verda, M. Santarelli, A. Sciacovelli, CSP plants with thermocline thermal energy storage and integrated steam generator – Techno-economic modeling and design optimization, *Energy.* 139 (2017) 231–246.
<https://doi.org/10.1016/j.energy.2017.07.160>.
- [34] P. Psarras, S. Comello, P. Bains, P. Charoensawadpong, S. Reichelsten, J. Wilcox, Carbon Capture and Utilization in the Industrial Sector, *Environ. Sci. Technol.* 51 (2017) 11440–11449.
- [35] Y. Yan, K. Wang, P.T. Clough, E.J. Anthony, Developments in calcium/chemical looping and metal oxide redox cycles for high-temperature thermochemical energy storage: A review, *Fuel Process. Technol.* 199 (2020) 106280.
<https://doi.org/10.1016/j.fuproc.2019.106280>.
- [36] C. Ortiz, M.C. Romano, J.M. Valverde, M. Binotti, R. Chacartegui, Process integration of Calcium-Looping thermochemical energy storage system in concentrating solar power plants, *Energy.* 155 (2018) 535–551.
<https://doi.org/10.1016/j.energy.2018.04.180>.
- [37] C.C. Cormos, Techno-economic implications of flexible operation for super-critical power plants equipped with

- calcium looping cycle as a thermo-chemical energy storage system, *Fuel*. 280 (2020) 118293. <https://doi.org/10.1016/j.fuel.2020.118293>.
- [38] A. MacKenzie, D.L. Granatstein, E.J. Anthony, J.C. Abanades, Economics of CO₂ capture using the calcium cycle with a pressurized fluidized bed combustor, *Energy and Fuels*. 21 (2007) 920–926. <https://doi.org/10.1021/ef0603378>.